

Markovian Reeb Graphs for Simulating Spatiotemporal Patterns of Life

Anantajit Subrahmanya¹, Chandrakanth Gudavalli¹, Connor Levenson¹, and B.S. Manjunath¹

¹ University of California, Santa Barbara, Santa Barbara, CA, USA

Abstract. Accurately modeling human mobility is critical for urban planning, epidemiology, and traffic management. In this work, we introduce Markovian Reeb Graphs, a novel framework that transforms Reeb graphs from a descriptive analysis tool into a generative model for spatiotemporal trajectories. Our approach captures individual and population-level Patterns of Life (PoLs) and generates realistic trajectories that preserve baseline behaviors while incorporating stochastic variability by embedding probabilistic transitions within the Reeb graph structure. We present two variants—Sequential Reeb Graphs (SRGs) for individual agents and Hybrid Reeb Graphs (HRGs) that combine individual with population PoLs, evaluated on the Urban Anomalies and Geolife datasets using five mobility statistics. Results demonstrate that HRGs achieve strong fidelity across metrics while requiring modest trajectory datasets without specialized side information. This work establishes Markovian Reeb Graphs as a promising framework for trajectory simulation with broad applicability across urban environments.

Keywords: Trajectory Clustering · Reeb Graphs · Patterns of Life

1 Introduction

Modeling human mobility patterns is essential for urban planning [1, 2], traffic management [3], energy allocation [4], public health [5], and disaster preparedness [5]. Mobile devices and location-based services have enabled large-scale GPS data collection [6, 7], but privacy restrictions and limited datasets hinder robust analysis and generalization. Even the largest publicly available datasets [8, 9] capture only a narrow slice of behavior, motivating the need for simulation frameworks to extrapolate from limited observations. Traditional simulation methods, such as Activity-Based Models (ABMs) [10] encode activity schedules and travel demand but require extensive calibration and high computational overhead, limiting scalability and adaptability. Deep learning approaches [10, 11] address some challenges by learning population-level mobility patterns from large datasets, but remain tied to specialized, high-volume data sources (e.g., financial transactions, social media check-ins), restricting their generalizability across urban environments and ability to generate trajectories for individual agents' Patterns of Life (PoLs). Recently, Reeb graphs have emerged as a promising method for analyzing geospatial trajectories [12]. Prior work showed that Temporal Reeb Graphs can partition trajectories into meaningful substructures for anomaly detection [13], suggesting

that Reeb graphs encode Patterns of Life. However, existing Reeb graph formulations are primarily discriminative: they detect deviations but cannot generate realistic trajectories or differentiate frequent from rare events.

Our key contribution is to transform Reeb graphs from an analysis tool into a generative framework. We introduce Markovian Reeb Graphs, which embed probabilistic transitions within the Reeb graph structure to model individual- and population-level mobility. This enables the generation of realistic future trajectories that preserve baseline PoLs while incorporating stochastic variability. Unlike ABMs, our method doesn't require extensive scenario-specific calibration, and unlike deep learning approaches, it can operate directly on modest trajectory datasets without specialized side information. This is the first work to unify topological representations of mobility with probabilistic modeling for scalable trajectory simulation.

We now summarize the key contributions of the paper:

1. We introduce Markovian Reeb Graphs, a data structure that captures individual and population-level Patterns of Life (PoLs).
2. We demonstrate how Reeb Graphs, traditionally an analytical tool, can be used in generative capacity for human mobility simulation.
3. We evaluate trajectories by Markovian Reeb Graphs on agent-level and population-level metrics both qualitatively and quantitatively.

2 Related Works

2.1 Past work on Reeb Graphs

Reeb graphs are structures that track changes in level set topology over a scalar function for shape analysis [14]. Recent scholarship adapted Reeb graphs for topological modeling of trajectories, such as neuronal fibers [15, 16] and human mobility patterns [12, 13], to summarize dense sequences as a sparse graph.

Previous work on geospatial trajectories has shown that Temporal Reeb Graphs (TERGs) can transform GPS points into nodes and edges to represent invariant subtrajectories for anomaly detection [13]. TERGs are constructed over time by defining nodes at points of change in the connected trajectories — when two or more trajectories transition from spatially disconnected to connected (a “connect” event) or vice versa (a “disconnect” event). Under this model, trajectories that disconnect from a Reeb graph are considered out of distribution, hence anomalous. The ability of TERGs to identify out of distribution points implies that Reeb graphs capture patterns of life (PoLs) and could simulate additional trajectories conforming to existing patterns of life for an individual agent. Reeb graphs’ utility beyond individual agent PoLs has also been explored Multi-Agent Reeb Graphs (MARGs), which capture population-level behaviors from multiple agents’ trajectories [12].

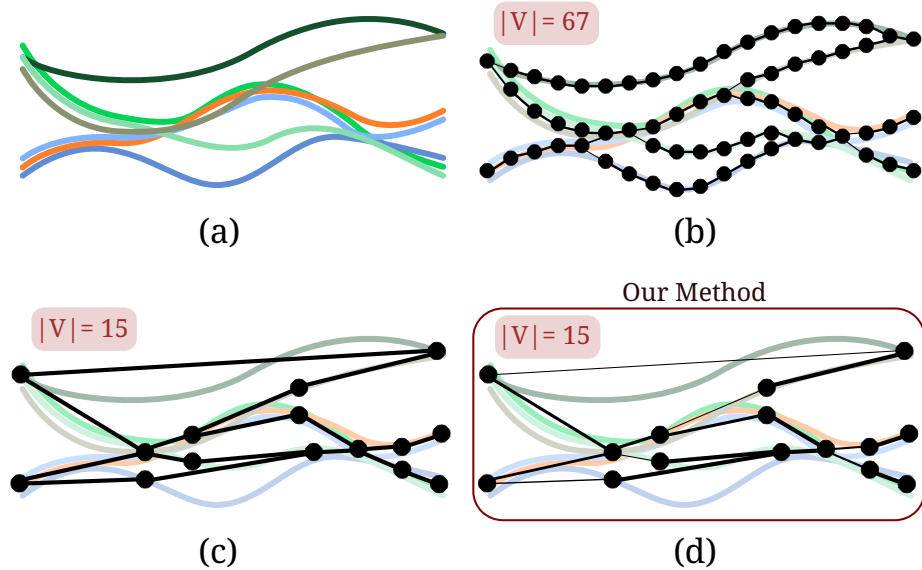


Fig. 1. Different graph representations of seven 1D (vertical axis: position, horizontal axis: time) trajectories (A), and their corresponding node counts $|V|$. (B) Time-Dependent Markov Chain constructed on trajectories with edge weight proportional to edge weight. (C) TEmporal Reeb Graph (TERG) constructed on trajectories at point of variance with low complexity but cannot differentiate between common/rare events. (D) Markovian Reeb Graphs efficiently capture both the points of variance and frequency of events.

Although MARGs and TERGs capture the possibility of an event occurring through connect and disconnect events, they cannot differentiate between frequent and infrequent events (Fig. 1C). Therefore, using existing Reeb graph data structures for human mobility simulation would confuse rare and daily behaviors, leading to unrealistic trajectories. Inspired by work modeling the human connectome [16], we introduce Markovian Reeb Graphs to resolve this limitation by including probabilities of a deviation in behavior through graph edge weights (Fig. 1D).

2.2 Past Work on Mobility Simulation Engines

Existing mobility simulation approaches broadly fall into routing engines, activity-based models (ABMs), and data-driven generative models. Routing engines simulate movement between specified start and end points, sometimes allowing

intermediate waypoints or transport-mode selection. For example, Valhalla [17] generates realistic point-to-point routes on real-world road networks, but does not model temporal activity patterns, agent-level variability, or higher-level behavioral rules. Similarly, SUMO [18] provides a detailed traffic simulation framework with fine-grained control over vehicle interactions and infrastructure, but requires extensive prior information like demand matrices and calibrated behavioral parameters, making large-scale deployment computationally intensive. In contrast, Markovian Reeb Graphs learn mobility dynamics from observed trajectories and generate new trajectories without requiring specialized side information or extensive calibration.

Activity-Based Models (ABMs) represent agents' daily schedules and decision-making processes [19]. Systems like MATSim optimize agents' plans through iterative utility maximization, while Patterns of Life Simulation frameworks incorporate behavioral heuristics like Maslow's hierarchy of needs [20, 21]. Although expressive, ABMs exhibit super-linear scaling with agent numbers and require substantial domain-specific input [19]. Recent deep generative models, including DeepAM [10], aim to reduce simulation costs by learning trip patterns from data; however, these approaches rely on large datasets and auxiliary information from surveys or existing simulators. Markovian Reeb Graphs can extrapolate individual and population-level mobility patterns from modest trajectory datasets.

To tackle data-collection and scalability challenges, recent methods learn urban mobility patterns from GPS trajectories using deep generative models [22]. Approaches like MoveSim [23] and DeepMobility [24] generate synthetic trajectories that match population-level statistics, evaluated using measures like distance traveled, radius of gyration, and travel duration. Markovian Reeb Graphs are competitive on these metrics while also enabling future trajectory simulation for existing agents based on their observed Patterns of Life.

Classical mobility models often rely on Markov chains [25]. In these models, states correspond to discrete spatial locations like points of interest [25–27]. While simple, these models do not capture route structure or fine-grained temporal dynamics [28]. Time-Varying Markov Chains (TVMCs) extend this formulation by allowing transition probabilities to depend on time of day [29]. However, they incur severe state-space growth with increased spatial and temporal resolution [30]. Markovian Reeb Graphs address this limitation by using topological abstraction to compress trajectories into a sparse graph that preserves temporal ordering, route structure, and transition frequencies. This yields a scalable generative model for agent-level and population-level mobility.

3 Methods

In this section, we describe how two types of Markovian Reeb Graphs can generate trajectories conforming to agent-level and population-level distributions. First, we introduce Sequential Reeb Graphs (SRGs), an improvement on TERGs that capture the frequency of behaviors in an individual agent's PoL. Next, we

introduce Hybrid Reeb Graphs (HRGs), which use Multi-Agent Reeb Graphs (MARGs) to generalize SRGs to represent population-level behaviors. Finally, we explain how either of these Markovian Reeb Graphs can generate trajectories.

3.1 Sequential Reeb Graph Construction (SRG)

A trajectory T is a sequence of (L) points p_0, p_1, \dots, p_{L-1} . Each $p_i \in T$ consists of (index, latitude, longitude) triplets. Each agent has N trajectories.

Two points $p_i = T_1[i]$ and $q_i = T_2[i]$ belong to a “bundle” (equivalence class) if $d(p_i, q_i) < \varepsilon$ for some metric d and threshold ε . For this paper, we assume d is the Euclidean distance between the latitude/longitude pairs. We define the set of bundles $B = \{b_1, b_2, \dots, b_M\}$. All points in a bundle $(p_a, p_b, \dots) \in b_i$ correspond to the same index across their source trajectories – let this quantity be defined as $\text{index}(b_i)$. Each bundle has a well-defined centroid, computed by averaging the components of the points within, defined as $\text{centroid}(b_i)$. Finally, we define the set of connected components (i.e. “connected” trajectories containing values in b_i as $\text{cc}(b_i) = \{k : T_k[\text{index}(b_i)] \in b_i\}$.

The nodes in an SRG are defined by changes in the sets of connected trajectories over the indices of the underlying trajectories. Each node $v \in V \subset B$ must satisfy $\text{cc}(v) \neq \text{cc}(b)$ for any $b \in B$ with $\text{index}(b) = \text{index}(v) - 1$. A bundle at index i is also a node if there’s no bundle in the previous index with the same connected components. Each directed edge in the Reeb graph from v_i to v_j satisfies $\text{cc}(v_i) \cap \text{cc}(v_j) \neq \emptyset$ with edge weight $w = \frac{|\text{cc}(v_i) \cap \text{cc}(v_j)|}{|\text{cc}(v_i)|}$. Intuitively, the edge weight represents the conditional probability that a trajectory is in bundle v_j given it was in bundle v_i .

Therefore, any SRG can be characterized by a set of N trajectories $A = \{T_1, T_2, \dots, T_N\}$ and two hyper-parameters: d (a distance metric) and ε (a scalar threshold).

Our algorithm for constructing SRGs has two phases, inspired by works on Reeb graphs for clustering spatiotemporal data [13]:

1. Bundle Computation: Compute a partition B such that each $b \in B$ forms a bundle defined by d and ε for all points across trajectories.
2. Reeb Graph Computation: Compute the subset $V \subset B$ and the set of edges $(v_i, v_j, w) \in V^2 \times [0, 1]$.

For computing bundles, we used an incremental algorithm [13] for bundle computation that uses R-trees (a spatial data structure) to organize the bundles. Once we computed the bundles, we used Algorithm 1 to compute the Reeb Graph. This algorithm has an average time complexity $O(LN \log(N) + |B|)$, where $|B|$ is the cardinality of the set of bundles B . This process introduces no additional overhead in Reeb graph computation compared to past works [13]. A more detailed discussion of the time complexity is in the Supplementary Material.

3.2 Population-Individual Hybrid Reeb Graphs

A Markovian Multi-Agent Reeb Graph (MARG) can capture population-level patterns using K agents $\{A_1, A_2, \dots, A_k\}$ with N trajectories each by concatenating the agents to create KN trajectories, each with length L : $M = \{T_1, T_2, \dots, T_{KN}\}$. It follows that the worst-case time complexity to compute a MARG is $O(LKN \log(KN))$. As with the SRG, the expected complexity scales log-linearly with the number of bundles, hence MARGs are faster to compute for groups of similar agents.

```

1 Initialize  $V \leftarrow \{\}, E \leftarrow \{\}$ 
2  $\text{states}[0][k] \leftarrow B[0][c]$  such that  $T_k \in \text{cc}(B[0][c])$ 
3 for  $i = 1$  to  $L - 1$  do
4    $\text{states}[i][k] \leftarrow B[i][c]$  such that  $T_k \in \text{cc}(B[i][c])$ 
5   for  $j = 1$  to  $N$  do
6     if  $\text{cc}(\text{states}[i][j]) \neq \text{cc}(\text{states}[i-1][j])$  or  $i = L - 1$ 
7       then
8         Add  $\text{states}[i][j]$  to  $V$  if not in  $V$ 
9         for  $T \in \text{cc}(\text{states}[i][j])$  do
10           Add edge  $(\text{states}[i-1][j], \text{states}[i][j], 0)$  to  $E$  if not
              in  $E$  with weight 0
11           Weight of  $(\text{states}[i-1][j], \text{states}[i][j])$  +=  $\frac{1}{\text{len}(\text{cc}(\text{states}[i-1][j]))}$ 

```

Algorithm 1. Algorithm for computing Sequential Reeb Graphs

Let $S(V_s, E_s)$ be the SRG of agent A_k , and let $M(V_m, E_m)$ be the population's MARG. We will fuse these graphs to create an HRG $H(V_h, E_h)$ for this agent. First, we find the corresponding nodes and edges between S and M . That is, for each node in V_s , we find the node with the nearest centroid in V_m – note that the nodes cannot differ by more than ε since A_k is represented in M . We draw an edge with weight α from each SRG node to its corresponding MARG node, and an edge with weight β from each MARG node to its corresponding SRG node. Intuitively, α represents the probability of an agent deviating from their PoL, and β represents the probability of reconnecting to their original Reeb graph. To anchor the HRG to A_k 's PoL, any node in H must have a path back to the agent SRG and any graph traversal must begin on the SRG for continuity between trajectories. Only the nodes and edges that satisfy both requirements were retained from M to H . A more detailed discussion of HRG construction and complexity is in Supplementary Material.

A critical limitation of a naive merge of an individual and population level graph is that if a traversal of the hybrid graph leaves the SRG, it may not

reconnect for many samples. This could lead to traversals drifting further from an agent's PoL. To account for this, we adjusted the weight of each edge in the HRG inversely proportional to the expected index (recall each bundle has an index) of return to the SRG. After all adjustments, the graph was traversed once to ensure the sum of outbound edge weights for every node is 1. Thus, the complexity of constructing the HRG is linear with respect to the nodes and edges in the MARG and SRG.

3.3 Trajectory Generation with Markovian Reeb Graphs

Sequential and Hybrid Reeb Graphs can generate trajectories through random node traversals in the Reeb Graph. Each edge (u, v) between two nodes of the Markovian Reeb Graph corresponds to a set of subtrajectories transitioning between critical points, $cc(u) \cap cc(v)$. We generate each subtrajectory by randomly picking one corresponding to the edge. This traversal continues, concatenating subtrajectories until a sink node (with no outbound edges) is reached.

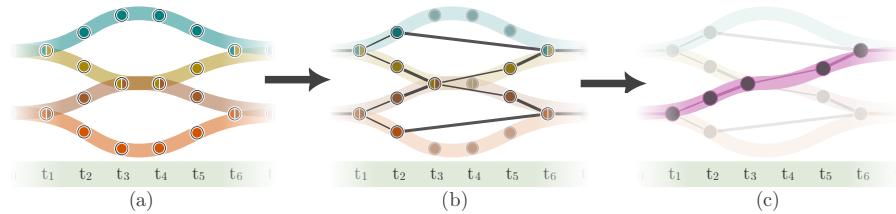


Fig. 2. Process of generating trajectories with Markovian Reeb Graphs. (a) Visualization of bundles (circles) for four trajectories. Two trajectories are “connected” if they overlap. The colors within each bundle represent the trajectories belonging to the bundle at each time step. (b) Sequential Reeb Graph computed from the bundles. Edge thickness corresponds to the edge weights. (c) A trajectory generated by the Sequential Reeb Graph. We generate a random traversal of the Reeb Graph’s nodes and edges, then copy a random subtrajectory corresponding to two edges. Concatenating all subtrajectories results in a new trajectory.

To generate a new trajectory using any Markovian Reeb Graph, we start with an empty trajectory $T = []$. We select the nearest source node to the endpoint of the previous trajectory to ensure continuity. In this paper, where each trajectory represents one day of mobility data, the end location of each day should match the start location of the next day. Next, we randomly select one of the outgoing edges of the chosen node, with the selection probability equal to its weight. We find the set of trajectories defining each node, say $cc(u)$ and $cc(v)$, and select one at random, say T_i . We copy the values of T_i corresponding to this edge, the subtrajectory $T_i[\text{index}(u) : \text{index}(v)]$, and append this to T . We continue this process, picking an edge from v until v is a sink node, at which point T should

have a length of L , since the only nodes with no outbound edges are at index L . The time complexity of generating each trajectory is linear with the maximum path length of the graph.

3.4 Markovian Reeb Graphs

Observe that the SRG defines states as bundles located at “critical points” where trajectory connectivity changes (nodes $v \in V$). The edge weights $w = \frac{|\text{cc}(v_i) \cap \text{cc}(v_j)|}{|\text{cc}(v_i)|}$ are empirical transition probabilities – the fraction of trajectories that transitioned from node v_i to v_j . Crucially, this probability depends only on the current state v_i , not on prior trajectory history, satisfying the memoryless property. Trajectory generation, as described in Section 3.3, performs a random walk: sample the next node according to edge weights then copy a random subtrajectory from $\text{cc}(v_i) \cap \text{cc}(v_j)$, and repeat. This constitutes a discrete-time acyclic Markov chain over state space V .

4 Experiments

4.1 Datasets

We evaluate our methods on two publicly available large-scale mobility datasets. For each dataset, we have a training subset (M1), an evaluation (M2) subset, the data generated by our method (G), and baseline data generated by a Mobility Markov Chain method (MMC) [25].

- Geolife [9]: A real-world dataset of 17,621 GPS trajectories from 182 users in Beijing over five years (April 2007 to August 2012), with varying trajectory lengths and sampling rates.
- Urban Anomalies (UA) [21]: A synthetic dataset with one month of normal data (M1) and one month of potentially anomalous data (M2) for agents in Atlanta or Berlin. Anomalous agents in M2 were removed, resulting in 28 days of data for 880 agents per subset, sampled every 5 minutes (approximately 7M points).

Sequential Reeb Graphs require uniformly sampled trajectories. To meet this requirement, Geolife trajectories were temporally resampled to a fixed interval using linear interpolation. Sparse segments were handled via a masking strategy to account for data dropout. Post-processing removed invalid samples to prevent dropout from influencing graph construction. For both datasets, M1 and M2 were defined so each subset contained a similar number of trajectories at a population level.

4.2 Evaluation Metrics

Following the practice in previous works [11, 28, 31], we define five statistics to evaluate our method’s performance: Daily Travel Distance: cumulative travel distance, Daily Travel Duration: number of moving samples, Longest Distance

Traveled: longest trip distance (or 0 if no trip present), Radius of Gyration: spatial range of movement, and New Locations Visited: number of unique stop points in M2/G/MMC not in M1.

We evaluated each statistic at the population and individual levels. The agent-level metrics were computed for M1, M2, and G, and compared against trajectories generated by Mobility Markov Chains (MMC) [25]. We computed the agent-wise mean and Mean Absolute Error between M1 and M2 and the generated data. The population-level metrics were generated similarly, except using a histogram with 100 bins on each statistic across all agents, then computed the Jensen-Shannon Divergence between the distributions. Together, these measure how well the generated trajectories adhere to each agent’s PoL and how well they conform to population Patterns of Life.

Due to the high dropout rate of the Geolife dataset, we computed distances on M1 and M2 on a subset of the time range with the most data points (roughly 5.5 hours) and retained agents with less than 15 consecutive minutes of dropout during this period in M1, M2 and G ($n = 24$) to ensure that agent-level statistics were meaningful. Finally, we filled in the missing timestamps with the last measured value, resampled to every 10 seconds.

Table 1. Agent and population metrics for data generated using three methods (SRG, HRG, MMC) on the Geolife dataset compared to M2, with nearest to M2 for each in **bold**.

Evaluation Statistic	Generation Method	Agent Score	Population Score
Distance Traveled	M2	0.04053	0.03816
	HRG	0.04569	0.05129
	SRG	0.04897	0.05129
	MMC	0.07414	0.05156
Duration of Movement	M2	35.62602	0.10754
	HRG	47.64929	0.15249
	SRG	64.36842	0.19429
	MMC	80.72590	0.336739
Longest Trip Distance	M2	16.10039	0.34872
	HRG	16.48089	0.36374
	SRG	16.59337	0.36374
	MMC	20.39080	0.33314
New Locations Visited	M2	1.03834	0.62800
	HRG	0.67179	0.26403
	SRG	0.00000	0.00000
	MMC	0.70549	0.58827
Radius of Gyration	M2	0.00669	0.03147
	HRG	0.00791	0.04865
	SRG	0.00831	0.04865
	MMC	0.00097	0.04431

It is important to recognize that lower MAE/JSD indicates stronger conformance with M1. However, lower values are not necessarily better because PoLs naturally evolve over time. Thus, MAE/JSD are evaluated by their similarity to M2, as marked in Table 1 and Table 2.

4.3 Results

Table 1 and Table 2 report results for SRG ($\varepsilon = 10^{-3}$) and HRG ($\varepsilon = 10^{-3}$, $\alpha = 1\%$, $\beta = 99.9\%$). We chose these hyperparameter values empirically; a sensitivity study is in Supplementary Material. Due to limited per-agent data in the Geolife dataset, we were only able to generate full trajectories for a subset of agents (those with at least one sample at each time of the day). We considered the M2 score as a baseline and marked the generation method (SRG, HRG) closer to the baseline M2 value. For Geolife, the HRG outperformed the SRG on all metrics. This may be due to the SRG lacking information to travel to all locations due to high dropout in M1, while the HRG can utilize MARG information to connect multiple disconnected locations. Compared to the baseline method (MCC), the HRG showed better performance on most metrics but fell slightly short on New Locations Visited and Radius of Gyration. In contrast, the Urban Anomalies dataset performance was closer. Both SRG and HRG performed similarly for distance traveled, longest trip distance, and radius of gyration. However, the HRG performed better in movement duration and new locations visited. Note that the latter is expected since SRGs cannot visit new locations not in M1. At this lower sampling rate without noise and dropout, both Markovian Reeb graph methods consistently outperformed MCC in both agent and population scores.

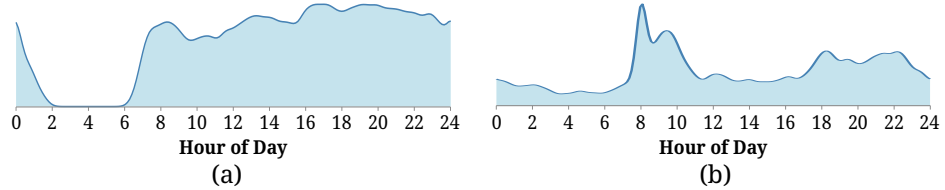


Fig. 3. Reeb Graph Statistics. Histograms show the density of nodes in the Urban Anomalies (A) and Geolife (B) dataset over hours. Geolife MARG was computed in UTC, but visualization is adjusted to UTC+8.

To understand Reeb Graphs intuitively, we can examine the node density over time (index) in the MARGs. We computed a histogram of the number of nodes for each time slice (indirectly a measure of variance) for both datasets. Then, we applied a Gaussian kernel to smooth the histograms to visualize the Reeb

graphs density over time. In the Urban Anomalies dataset, there are no nodes between 2am and 6am. As agents “wake up” around 6am, the number of nodes ramps up. There are peaks at 8am (going to work), 1pm (lunch), 5pm (leaving work), and 6pm (dinner) — however, the number of nodes during the movement period is consistently high (Fig. 3A). In the Geolife dataset, agents have more realistic behavior variability. The initial peak at 8am is an artifact of Reeb graph construction since a node is created if it is present at the start and end of the trajectories. We observe a peak near 9am, presumably agents going to work, with little variation throughout the day (agents do not leave work). Near the end of the day, there is an increase in variance as agents leave work, followed by decaying node counts as they return home (Fig. 3B). We acknowledge these trends in the Geolife dataset may be influenced by dropout (nodes influenced by the start and end of dropout periods).

Table 2. Agent and population metrics for data generated using three methods (SRG, HRG, MMC) on the UA dataset compared to M2, with nearest to M2 for each in **bold**.

Evaluation Statistic	Generation Method	Agent Score	Population Score
Distance Traveled	M2	0.00972	0.03891
	HRG	0.00406	0.20935
	SRG	0.00401	0.20451
	MMC	0.04700	0.42560
Duration of Movement	M2	1.53693	0.04087
	HRG	1.16636	0.28211
	SRG	0.65946	0.27314
	MMC	7.40524	0.54722
Longest Trip Distance	M2	0.04276	0.16495
	HRG	0.09806	0.42455
	SRG	0.09750	0.42416
	MMC	0.18481	0.71763
New Locations Visited	M2	0.00081	0.01677
	HRG	0.00057	0.01403
	SRG	0.00000	0.00000
	MMC	0.66305	0.56807
Radius of Gyration	M2	0.00034	0.02781
	HRG	0.00073	0.17383
	SRG	0.00073	0.17381
	MMC	0.00425	0.40035

Promising qualitative and quantitative trajectory generation performance indicated that the MARG of a population may capture sufficient information on the region’s dynamics. To demonstrate the richness of information captured, we queried the MARG built on the Geolife dataset to simulate paths between locations. First, we computed the most probable traversal between the two nodes.

Then, we applied a similar trajectory generation algorithm to generate a continuous trajectory. The resulting trajectory doesn't exist in the dataset, yet includes low-level behaviors like using multiple modes of transport (Fig. 4A), slowing down at intersections (Fig. 4B) and navigating one-way streets (Fig. 4C). Although encouraging, this should be treated as a preliminary exploration in the routing engine space and further research is needed to make any major claims.

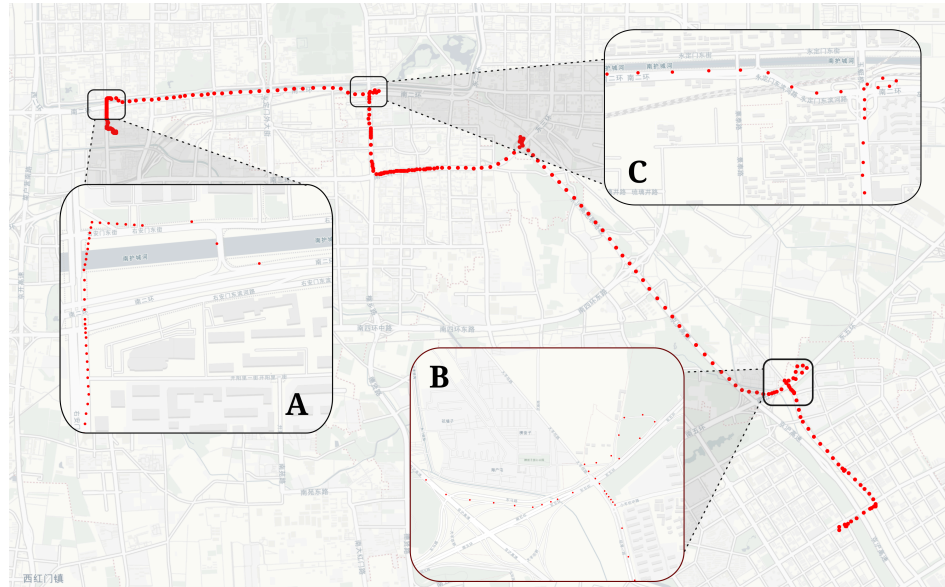


Fig. 4. An example trajectory generated using MARGs as a routing method. The algorithm was given two coordinates, a start time (9am), and an end time (10:30am). (A) Agent switches mode of transit, perhaps dismounting from a bus at the bus stop. (B) Agent slows down before crossing an intersection. (C) Agent navigates one-way roads and a roundabout.

4.4 Reproducibility Statement

All methods to reproduce every figure, table, and result in this paper are open source and well documented at <https://github.com/anantajit/MarkovReeb>. The two datasets used are publicly available [9, 21].

5 Conclusion

In this paper, we introduced Markovian Reeb Graphs as a generative framework for modeling human mobility. Through Sequential and Hybrid variants, we

demonstrated how Reeb graphs can simulate realistic trajectories that preserve individual- and population-level Patterns of Life. Our evaluation on the Urban Anomalies and Geolife datasets showed that Hybrid Reeb Graphs achieve the best balance across agent- and population-level metrics on simulated and real-world data. However, in cases with limited population information, Sequential Reeb Graphs perform competitively as well. We also briefly explored using Markovian Reeb Graphs to generate realistic multi-modal routes between locations.

Markovian Reeb Graphs show strong performance, but several limitations and opportunities for extension remain. The primary constraint is that trajectories can only connect when spatially proximate at aligned time indices. This may induce false disconnects under low sampling rates or high agent velocities, though this is mitigated with dense data as seen in Geolife. The framework may struggle to accurately model rare or unseen behaviors, particularly in small populations where transitions are weakly supported. Hybrid Reeb Graphs partially address this by incorporating population-level structure, but require at least one existing sample to generate each behavior. Additionally, our work does not account for POI semantics or alternative periodicities (weekly, monthly, etc.) beyond daily routines, and our evaluation is limited by real-world data availability. Future work includes incorporating semantic or latent embeddings for POIs [32], improving robustness to sparse and noisy GPS data, modeling longer-term periodic behaviors, and assigning likelihoods for applications such as anomaly detection. Further exploration of temporally-aware path construction using MARGs may unlock new applications in simulation and controlled out-of-distribution behavior generation. Collectively, these directions position Markovian Reeb Graphs as a flexible and promising foundation for realistic mobility synthesis.

References

1. Zhang, J., Feng, B., Wu, Y., Xu, P., Ke, R., Dong, N.: The effect of human mobility and control measures on traffic safety during COVID-19 pandemic. *PLOS ONE*. 16, e243263 (2021). <https://doi.org/10.1371/journal.pone.0243263>.
2. Keenan, J.M., Ajibade, I., Tietjen, B.C.: The state of planning, policy, and justice for human mobility in national adaptation plans. *Earth System Governance*. 25, 100266 (2025). <https://doi.org/10.1016/j.esg.2025.100266>.
3. Hoppe, J., Schwinger, F., Haeger, H., Wernz, J., Jarke, M.: Improving the Prediction of Passenger Numbers in Public Transit Networks by Combining Short-Term Forecasts With Real-Time Occupancy Data. *IEEE Open Journal of Intelligent Transportation Systems*. 4, 153–174 (2023). <https://doi.org/10.1109/OJITS.2023.3251564>.
4. Mohammadi, N., Taylor, J.E.: Urban Energy Flux: Human Mobility as a Predictor for Spatial Changes, <http://arxiv.org/abs/1609.01239>, last accessed 2025/08/05. <https://doi.org/10.48550/arXiv.1609.01239>.
5. Lai, S., Farnham, A., Ruktanonchai, N.W., Tatem, A.J.: Measuring mobility, disease connectivity and individual risk: a review of using mobile phone data and mHealth for travel medicine. *Journal of Travel Medicine*. 26, taz19 (2019). <https://doi.org/10.1093/jtm/taz019>.

6. Draijer, G., Kalfs, N., Perdok, J.: Global Positioning System as Data Collection Method for Travel Research. *Transportation Research Record*. 1719, 147–153 (2000). <https://doi.org/10.3141/1719-19>.
7. Yabe, T., Tsubouchi, K., Shimizu, T., Sekimoto, Y., Sezaki, K., Moro, E., Pentland, A.: Metropolitan Scale and Longitudinal Dataset of Anonymized Human Mobility Trajectories. *CoRR*. (2023).
8. Yabe, T., Tsubouchi, K., Shimizu, T., Sekimoto, Y., Sezaki, K., Moro, E., Pentland, A.: YJMob100K: City-scale and longitudinal dataset of anonymized human mobility trajectories. *Scientific Data*. 11, 397 (2024). <https://doi.org/10.1038/s41597-024-03237-9>.
9. Zheng, Y., Xie, X., Ma, W.-Y.: GeoLife: A Collaborative Social Networking Service among User, location and trajectory. *IEEE Data(base) Engineering Bulletin*. (2010).
10. Liao, X., Jiang, Q., He, B.Y., Liu, Y., Kuai, C., Ma, J.: Deep Activity Model: A Generative Approach for Human Mobility Pattern Synthesis, <http://arxiv.org/abs/2405.17468>, last accessed 2025/07/31. <https://doi.org/10.48550/arXiv.2405.17468>.
11. Kim, J.-S., Thakur, G.M., Amichi, L., Burger, A., Gunaratne, C., Tuccillo, J., Hauser, T., Bentley, J., Sparks, K., De, D., Brown, C., McBride, E., McGaha, J., Gaboardi, J., Nie, X., Christopher, S.C.: HumoNet: A Framework for Realistic Modeling and Simulation of Human Mobility Network. In: 2024 25th IEEE International Conference on Mobile Data Management (MDM). pp. 185–194 (2024). <https://doi.org/10.1109/MDM61037.2024.00042>.
12. Gudavalli, C., Zhang, B., Levenson, C., Lore, K.G., Manjunath, B.S.: ReeFRAME: Reeb Graph based Trajectory Analysis Framework to Capture Top-Down and Bottom-Up Patterns of Life. Presented at the October (2024). <https://doi.org/10.1145/3681765.3698452>.
13. Zhang, B., Shailja, S., Gudavalli, C., Levenson, C., Khan, A., Manjunath, B.S.: ReeSPOT: Reeb Graph Models Semantic Patterns of Normalcy in Human Trajectories, <http://arxiv.org/abs/2405.00808>, last accessed 2025/07/27. <https://doi.org/10.48550/arXiv.2405.00808>.
14. Sun, J., Cieslak, M., Grafton, S., Suri, S.: A reeb graph approach to tractography. In: Proceedings of the 23rd SIGSPATIAL International Conference on Advances in Geographic Information Systems. pp. 1–4. Association for Computing Machinery, New York, NY, USA (2015). <https://doi.org/10.1145/2820783.2820848>.
15. Shailja, S., Grafton, S.T., Manjunath, B.S.: A robust Reeb graph model of white matter fibers with application to Alzheimer’s disease progression★, <https://www.biorxiv.org/content/10.1101/2022.03.11.482601v1>, last accessed 2025/08/15. <https://doi.org/10.1101/2022.03.11.482601>.
16. Shailja, S., Bhagavatula, V., Cieslak, M., Vettel, J.M., Grafton, S.T., Manjunath, B.S.: ReeBundle: A Method for Topological Modeling of White Matter Pathways Using Diffusion MRI. *IEEE Transactions on Medical Imaging*. 42, 3725–3737 (2023). <https://doi.org/10.1109/TMI.2023.3306049>.
17. valhalla/valhalla, <https://github.com/valhalla/valhalla>, last accessed 2025/08/16.
18. Stanford, C., Adari, S., Liao, X., He, Y., Jiang, Q., Kuai, C., Ma, J., Tung, E., Qian, Y., Zhao, L., Zhou, Z., Rasheed, Z., Shafique, K.: NUMOSIM: A Synthetic Mobility Dataset with Anomaly Detection Benchmarks, <http://arxiv.org/abs/2409.03024>, last accessed 2025/07/31. <https://doi.org/10.48550/arXiv.2409.03024>.
19. Lam, H.Y., Jayasinghe, S., Ahuja, K.D.K., Hills, A.P.: Agent-based modelling in active commuting research: a scoping review. *Critical Public Health*. 35, 2483473 (2025). <https://doi.org/10.1080/09581596.2025.2483473>.
20. Amiri, H., Kohn, W., Ruan, S., Kim, J.-S., Kavak, H., Crooks, A., Pfofer, D., Wenk, C., Züfle, A.: The Patterns of Life Human Mobility Simulation. In: Proceedings of the

32nd ACM International Conference on Advances in Geographic Information Systems. pp. 653–656. Association for Computing Machinery, New York, NY, USA (2024). <https://doi.org/10.1145/3678717.3691319>.

- 21. Amiri, H., Kong, R., Züffle, A.: Urban Anomalies: A Simulated Human Mobility Dataset with Injected Anomalies. In: Proceedings of the 1st ACM SIGSPATIAL International Workshop on Geospatial Anomaly Detection. pp. 1–11. Association for Computing Machinery, New York, NY, USA (2024). <https://doi.org/10.1145/3681765.3698459>.
- 22. Chen, X., Xu, J., Zhou, R., Chen, W., Fang, J., Liu, C.: TrajVAE: A Variational AutoEncoder model for trajectory generation. *Neurocomputing*. 428, 332–339 (2021). <https://doi.org/10.1016/j.neucom.2020.03.120>.
- 23. Feng, J., Yang, Z., Xu, F., Yu, H., Wang, M., Li, Y.: Learning to Simulate Human Mobility. In: Proceedings of the 26th ACM SIGKDD International Conference on Knowledge Discovery & Data Mining. pp. 3426–3433. Association for Computing Machinery, New York, NY, USA (2020). <https://doi.org/10.1145/3394486.3412862>.
- 24. Yuan, Y., Ding, J., Jin, D., Li, Y.: Learning the complexity of urban mobility with deep generative network. *PNAS Nexus*. 4, pgaf81 (2025). <https://doi.org/10.1093/pnasnexus/pgaf081>.
- 25. Gambs, S., Killijian, M.-O., Prado Cortez, M.N. del: Next place prediction using mobility Markov chains. In: Proceedings of the First Workshop on Measurement, Privacy, and Mobility. pp. 1–6. Association for Computing Machinery, New York, NY, USA (2012). <https://doi.org/10.1145/2181196.2181199>.
- 26. Kim, H., Song, H.Y.: Formulating Human Mobility Model in a Form of Continuous Time Markov Chain. *Procedia Computer Science*. 10, 389–396 (2012). <https://doi.org/10.1016/j.procs.2012.06.051>.
- 27. Yan, M., Li, S., Chan, C.A., Shen, Y., Yu, Y.: Mobility Prediction Using a Weighted Markov Model Based on Mobile User Classification. *Sensors* (Basel, Switzerland). 21, 1740 (2021). <https://doi.org/10.3390/s21051740>.
- 28. Lin, H., Shaham, S., Chiang, Y.-Y., Shahabi, C.: Generating Realistic and Representative Trajectories with Mobility Behavior Clustering. In: Proceedings of the 31st ACM International Conference on Advances in Geographic Information Systems. pp. 1–4. Association for Computing Machinery, New York, NY, USA (2023). <https://doi.org/10.1145/3589132.3625657>.
- 29. Wang, H., Zeng, S., Li, Y., Jin, D.: Predictability and Prediction of Human Mobility Based on Application-Collected Location Data. *IEEE Transactions on Mobile Computing*. 20, 2457–2472 (2021). <https://doi.org/10.1109/TMC.2020.2981441>.
- 30. Apers, S., Sarlette, A., Ticozzi, F.: Characterizing limits and opportunities in speeding up Markov chain mixing. *Stochastic Processes and their Applications*. 136, 145–191 (2021). <https://doi.org/10.1016/j.spa.2021.03.006>.
- 31. Zhu, Y., Ye, Y., Wu, Y., Zhao, X., Yu, J.: SynMob: Creating High-Fidelity Synthetic GPS Trajectory Dataset for Urban Mobility Analysis. *Advances in Neural Information Processing Systems*. 36, 22961–22977 (2023).
- 32. Li, Z., Kim, J., Chiang, Y.-Y., Chen, M.: SpaBERT: A Pretrained Language Model from Geographic Data for Geo-Entity Representation. Findings of the Association for Computational Linguistics: EMNLP 2022. (2022).